Evidence for Direct *trans* Insertion in a Hydrido–Olefin Rhodium Complex—Free Nitrogen as a Trap in a Migratory Insertion Process

Arkadi Vigalok, Heinz-Bernhard Kraatz, Leonid Konstantinovsky, and David Milstein*

Abstract: Reduction of the hydrido chloride complex [Rh(H)Cl{$CH_3C(CH_2CH_2P(tBu)_2)_2$}] (**4**) with NaH under a nitrogen atmosphere results in formation of two products: the dinitrogen complex [Rh(N_2)-{$CH_3C(CH_2CH_2P(tBu)_2)_2$}] (**2**) and the unusual low-valent hydrido–olefin complex, [RhH{CH_2=$C(CH_2CH_2P(tBu)_2)_2$}] (**3**). In the presence of N_2, complexes **2** and **3** are in equilibrium in solution; **2** is about 2.9 kcal mol^{-1} more stable than **3** + N_2. Both complexes co-crystallize in the solid state; they occupy the same crystallographic site in the crystal lattice ($P2_1/c$; $Z = 4$; $a = 12.173(2)$, $b = 14.121(3)$, $c = 15.367(3)$; $\alpha = 90$, $\beta = 106.50(3)$, $\gamma = 90°$). The mechanism of the reversible interconversion of **2** and **3** has been studied in detail. Complex **3** undergoes rapid olefin insertion/β-hydrogen elimination processes. The insertion rates were measured at different temperatures by saturation transfer NMR experiments, providing evidence for a highly organized late transition state ($\Delta S^{\neq} \approx -40$ e.u.), which can be caused by a concerted "*trans* migration". This theoretically unfavorable process is assisted by a distortion from the ideal square-planar configuration, including a decrease of the P-Rh-P angle and some bias of the double bond toward the hydride as indicated by the X-ray crystal structure of **3**. Under a nitrogen atmosphere, the intermediate formed upon olefin insertion is slowly trapped by free dinitrogen to form complex **2**. The dinitrogen dissociation from **2** was found to be the rate-determining step for the overall interconversion of **2** and **3** ($\Delta G^{\neq}_{298} = 24.1$ kcal mol^{-1}).

Keywords
dinitrogen · hydrido complexes · insertions · olefins · rhodium

Introduction

Insertion of coordinated olefins into metal–hydride bonds, together with its microscopic reverse β-hydrogen elimination, are among the most fundamental processes in organometallic chemistry and much has been done to evaluate the thermodynamic and kinetic parameters of this important class of reaction, which play a key role in major catalytic processes.[1] However, one of the limitations of these studies is the instability of hydrido–olefin complexes of transition metals. Most of the information was obtained with saturated early transition metal complexes[2] or late transition metal complexes in high oxidation states,[3] which are normally more stable. Much less is known about *low-valent, unsaturated* late transition metal complexes with hydride and olefin ligands.[4] All of the reported examples involve *cis* insertion.

We have recently demonstrated that bulky P-C-P type ligands can stabilize electron-rich, low-valent rhodium complexes **1** with various loosely bound gaseous molecules.[5] Since it is well known that unsaturated electron-rich late transition metal complexes easily undergo β-hydrogen elimination,[6, 7] we were interested in the synthesis of complex **2**, which may form the hydrido–olefin complex **3** upon the dissociation of the dinitrogen molecule. Indeed, we obtained complexes **2** and **3** and observed that they undergo reversible interconversion. Our study of the thermodynamics and kinetics of the reactions involved in this overall equilibrium provided the first example of direct *trans* insertion of an olefin into an M–H bond, without prior isomerization into the *cis* complex. Even in very low concentrations in solution, atmospheric dinitrogen exerts a major effect on this process.

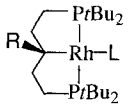

1: R=H, L=N_2 (a), H_2 (b), C_2H_4 (c), CO_2 (d);
2: R=CH_3, L=N_2.

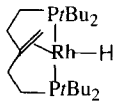

3

Results

1. Preparation of complexes 2 and 3: We have recently demonstrated that, in the presence of a large excess of sodium hydride under a nitrogen atmosphere, it is possible to eliminate HCl from a rhodium hydrido chloride complex and obtain the new

[*] D. Milstein, A. Vigalok, H.-B. Kraatz, L. Konstantinovsky
Department of Organic Chemistry, The Weizmann Institute of Science
Rehovot 76100 (Israel)
e-mail: comilst@weizmann.weizmann.ac.il

dinitrogen complex **1a**. However, when complex **4**[8] was treated with an excess of NaH in THF, two products, **2** and **3**, were obtained after evaporation of the solvent and extraction with pentane (Scheme 1). According to the NMR data, the ratio

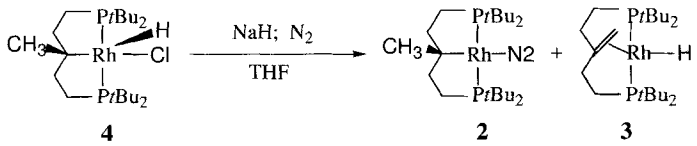

4 **2** **3**

Scheme 1.

between **2** and **3** was independent of the reaction time and equaled approximately 1:1. No other species was observed, even upon cooling to −70 °C. Both complexes are highly soluble in pentane and could not be separated by fractional crystallization. However, complex **3** was obtained analytically pure by passing argon through the solution (vide infra).

2. Characterization of complex 2: Complex **2** is an air-sensitive solid. The dinitrogen ligand displays a very characteristic strong IR absorption band at $\tilde{\nu} = 2110\ cm^{-1}$ (film). The same absorption is observed in solution (cyclohexane, benzene, dioxane). This frequency is similar to the one observed for the analogous complex **1a**.[5] Upon passing argon through a solution of **2**, this signal disappears and it reappears after exposure to a nitrogen atmosphere; this result indicates the presence of an equilibrium involving dinitrogen dissociation.

The $^{31}P\{^1H\}$ NMR spectrum of **2** in C_6D_6 shows a doublet at $\delta = 86.95$ with $J(Rh-P) = 172.1$ Hz. In the ^1H NMR spectrum, the methyl group is not coupled to Rh and P and it appears as a singlet at $\delta = 1.16$. The protons of the *t*Bu groups give rise to two sets of virtual triplets centered at $\delta = 1.3$ and 1.28. The $^{13}C\{^1H\}$ NMR spectrum also shows two different signals due to the *t*Bu groups. The *ipso* carbon appears as a doublet of triplets at $\delta = 55.6$ ($J(Rh-C) = 28.1$ Hz, $J(P-C) = 1.9$ Hz), and the methyl group bound to the *ipso*-C gives rise to a singlet at $\delta = 27.66$.

3. Characterization of complex 3: An analytically pure sample of complex **3** was obtained by passing dry argon through a warm solution containing **2** and **3** in benzene. The IR spectrum of complex **3** exhibits a broad Rh–H band at 1791 cm^{-1} (film), which is very unusual for rhodium hydride complexes. This very large shift to lower energy indicates the presence of a ligand with a strong *trans* influence in a position *trans* to the hydride.[9] Similar frequencies have been obtained with iridium *trans* dihydride complexes.[10] We believe that this lowering of the rhodium–hydride frequency may be caused by rhodium "slippage" towards the quaternary carbon, giving the ligand *trans* to the hydride an "alkyl-like" character.

The chemical shift of the hydride in the ^1H NMR spectrum ($\delta = -3.16$, dt, $J(Rh-H) = 21.0$ Hz) is also at a much lower field than that expected for a rhodium hydride, which usually appears upfield of $\delta = -8$. A 2D long-range coupling-enhancing COSY experiment showed a very weak cross-signal due to spin–spin interaction between the hydride and the olefin protons. No Overhauser effect was observed at low temperatures between these nuclei.

The olefin protons of complex **3** appear as a broad (8 Hz) singlet at $\delta = 2.78$ in the ^1H NMR spectrum. No coupling with rhodium or phosphorus was observed. This chemical shift is slightly downfield from the one reported for the analogous chloride complex $[RhCl\{CH_2{=}C(CH_2CH_2P(tBu)_2)_2\}]$.[8]

The $^{13}C\{^1H\}$ NMR spectrum of **3** unambiguously confirms the presence of the alkene ligand, exhibiting two doublets of triplets at $\delta = 97.4$ ($J(Rh-C) = 9.8$ Hz, quaternary carbon) and at $\delta = 48.22$ ($J(Rh-C) = 8.6$ Hz, methylene group). The latter overlaps with the signal of the (CH_2CH_2P) groups. The higher Rh–C coupling constant for the quaternary carbon versus the carbon of the CH_2 group suggests that the rhodium atom has slipped towards the former.

The $^{31}P\{^1H\}$ NMR spectrum shows a doublet at $\delta = 86.71$ with $J(Rh-P) = 152.7$ Hz, confirming the symmetrical positioning of the phosphorus atoms *trans* to each other in solution. The position of the signal is dramatically shifted downfield (more than 20 ppm) from that of the analogous chloride complex $[RhCl\{CH_2{=}C(CH_2CH_2P(tBu)_2)_2\}]$. Trogler et al. observed a large downfield shift of the phosphorus signal of a palladium hydride complex relative to those of the analogous palladium chloride, methyl, or BF_4 complexes.[11]

4. Equilibrium study: Complexes **2** and **3** undergo reversible, temperature-dependent interconversion in solution. When a 1:1 solution of **2** and **3** in benzene is heated to 80 °C, complex **2** is totally converted into **3**, as observed by $^{31}P\{^1H\}$ NMR, with no other products formed. When this solution is cooled to room temperature under an atmosphere of nitrogen, **2** is slowly formed until the mixture reaches the equilibrium ratio between complexes **2** and **3** (approximately 1:1) (Scheme 2).

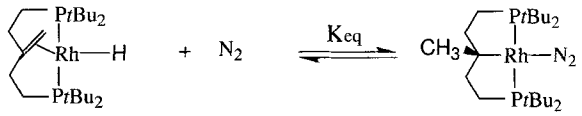

3 **2**

Scheme 2.

Equilibrium parameters were derived from experiments carried out at different temperatures. In a typical experiment, a solution of **2** and **3** was allowed to reach a given temperature and was then held at this temperature until an equilibrium was established, as observed by $^{31}P\{^1H\}$ NMR spectroscopy (usually about 30 min). The equilibrium constants were calculated from Equation (1), where $[N_2]$ is the equilibrium concentration of dinitrogen in benzene at the given temperature, as deduced from literature data.[12]

$$K_{eq} = \frac{[2]}{[3][N_2]} \quad (1)$$

Figure 1 shows the temperature dependence of the equilibrium in Scheme 2, which yields a ΔH of -7.53 kcal mol^{-1} and a ΔS of -15.5 e.u. The equilibrium constants and ΔG of the reaction at different temperatures are presented in Table 1.

It can be seen that formation of the dinitrogen complex **2** from complex **3** is quite favorable, ΔG for the equilibrium in Scheme 2 at 21 °C being approximately -3 kcal mol^{-1}. In an

0947-6539/97/0302-0254 $ 15.00+.25/0 Chem. Eur. J. 1997, 3, No. 2

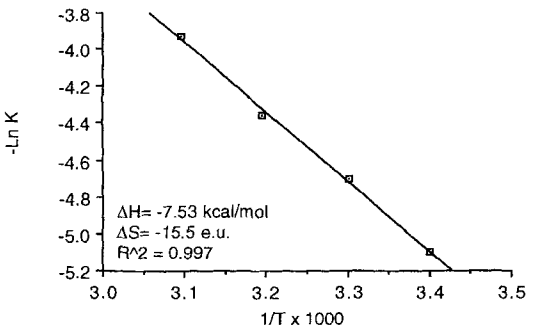

Figure 1. Temperature dependence of the equilibrium in Scheme 2.

Table 1. Temperature dependence of the equilibrium in Scheme 2.

T/°C	K_{eq}	ΔG/kcal mol^{-1}
21	163.69	−2.978
30	110.06	−2.830
40	77.94	−2.709
50	50.60	−2.518

analogous system, we have already shown that dinitrogen is quite a good ligand, capable of stabilizing an unsaturated electron-rich rhodium complex even better than ethylene.[5] Similar thermodynamic parameters were also obtained in dioxane.[13]

Interestingly, pressurizing an equilibrium mixture of **2** and **3** in cyclohexane or benzene with nitrogen (80 psi) at room temperature in a high-pressure NMR tube for a few hours resulted in the complete disappearance of **3** and practically quantitative formation of **2**. *To our knowledge this is the first example of an overall migratory insertion process influenced by* N_2. Release of the extra pressure of N_2 re-establishes the corresponding equilibrium ratio between **2** and **3**.

5. Kinetic studies: The equilibrium between complexes **2** and **3** in solution provides an opportunity to study the kinetics of the hydride migration to the olefin by NMR. An NOE difference experiment at room temperature gave a slightly negative value for the signal from the olefinic protons upon saturation of the hydride signal.[14] Similarly, saturation of the signal from the olefin gave about the same negative NOE for the hydride signal. The negative NOE increased as the temperature increased. These phenomena in our system are caused exclusively by a chemical exchange. Therefore, one must be very cautious in the interpretation of NOE data as a measure of through-space interactions unless the absence of exchange between the two nuclei has been proved.

In order to evaluate k_1 for the equilibrium shown in Scheme 3,[15] saturation-transfer experiments were performed between 40 and 70 °C. At lower temperatures, the process proceeds too slowly for the application of this technique.

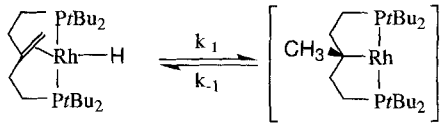

3 **5**

Scheme 3.

When an equilibrium mixture of **2** and **3** in C_6D_6 was heated, C–D bond activation took place, resulting in H/D exchange of the olefin protons and of the hydride. This caused broadening of the signals in ^{1}H NMR and the appearance of additional splitting in the hydride region. This problem was avoided by using [D_8]dioxane as a solvent; no changes in the spectra were observed when the complexes were heated in dioxane at 70 °C for several hours. All the measurements were carried out under equilibrium conditions, as determined by $^{31}P\{^1H\}$ NMR spectroscopy. Complex **5** was not observed throughout the experiments, indicating that $k_{-1} \gg k_1$ under the experimental conditions. The response of the signal of the olefinic protons upon saturation of the hydride (saturation transfer difference) at various temperatures is shown in Figure 2.

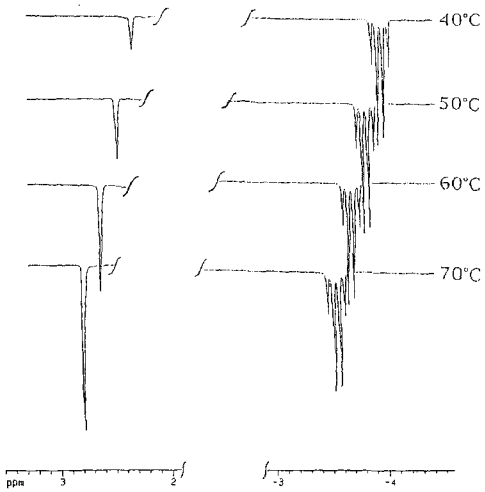

Figure 2. Response of the olefinic protons upon the saturation of the hydride in **3** at different temperatures (saturation transfer difference). The δ scale corresponds to that in the lowest spectrum.

The exchange rate constants k_{obs} were calculated by means of the Forsen–Hoffman equation[16] (see Experimental Section). The rate constants k_1 were calculated taking into consideration the difference in the spin population between the exchanging nuclei.[17] The rate constants and the kinetic parameters, derived from the Eyring equation, are presented in Table 2. The Eyring plot for the equilibrium in Scheme 3 is given in Figure 3. The high negative value for the entropy of activation of −39.3 e.u. indicates the presence of a concerted, highly organized transition state (see Discussion).

Significantly, saturation of the hydride signal at 50 °C had no effect on the signal of the methyl group in **2**. Also, no effect on the hydride or the olefinic protons in **3** was observed upon

Table 2. Rate constants and activation parameters for the equilibrium shown in Scheme 3.

T/°C	k_1/s^{-1}	$\Delta G^{\ddagger}_{298}$/kcal mol^{-1}	$\Delta H^{\ddagger}$/kcal mol^{-1}	$S^{\ddagger}$/e.u.
40	0.197			
50	0.305	18.8	7.1	−39.3
60	0.452			
70	0.575			

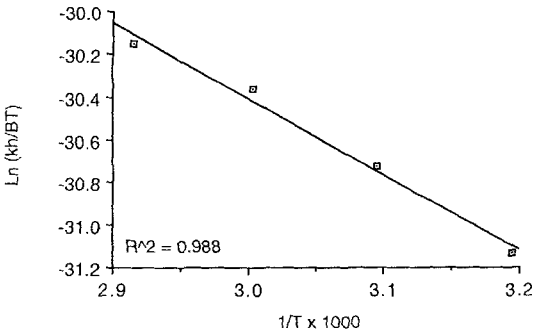

Figure 3. Eyring plot of the reaction in Scheme 3.

saturation of the methyl protons in **2**. This indicates that trapping of the 14-electron intermediate **5** by a nitrogen molecule has a substantially higher activation barrier than that of the β-hydrogen elimination process and, therefore, dissociation of N_2 from **2** is the rate-determining step for the overall conversion of **2** to **3**.

In order to quantify the rates of N_2 dissociation and reassociation, a kinetic study of the conversion of **2** into **3** was performed. A benzene solution containing complexes **2** and **3** at 25 °C was pressurized with 80 psi of N_2 in a high-pressure NMR tube; this resulted in practically quantitative conversion of **3** into **2** (see above). Upon release of the pressure, complex **2** was slowly converted into **3**. By using $^{31}P\{^1H\}$ NMR spectroscopy to monitor the rate of disappearence of **2** and formation of **3**, the reaction was shown to have a first-order dependence on the concentration of **2**, with $k_{obs} = 1.2(\pm 0.2) \times 10^{-5}\ s^{-1}$ (Figure 4).

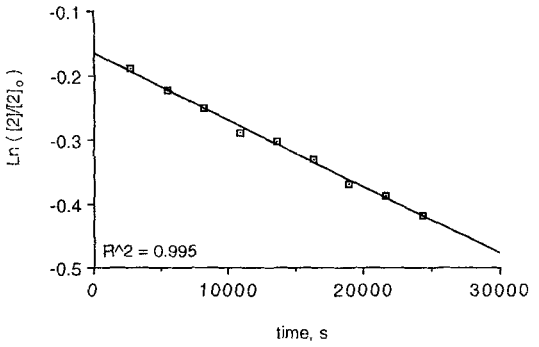

Figure 4. First-order kinetic fit for the disappearance of **2**.

Since the intermediate **5** could not be observed under any conditions, the steady-state approximation was applied for reaction (2). Due to the low dinitrogen solubility in benzene

$$\mathbf{2} \underset{k_2}{\overset{k_{-2}}{\rightleftharpoons}} \mathbf{5} + N_2 \qquad \mathbf{5} \underset{k_1}{\overset{k_{-1}}{\rightleftharpoons}} \mathbf{3} \tag{2}$$

(≈ 0.005 M) and high prevalence in concentration of complex **2** over **3** at the beginning of the experiment, the rate Equation (3) can be simplified into Equation (4). Therefore, the dinitrogen

$$\frac{d[\mathbf{3}]}{dt} = k_{-1}\frac{k_2[\mathbf{2}] + k_1[\mathbf{3}]}{k_{-1} + k_2[N_2]} - k_1[\mathbf{3}] \tag{3}$$

$$\frac{d[\mathbf{3}]}{dt} = k_{-2}[\mathbf{2}] \tag{4}$$

dissociation rate constant k_{-2} becomes equal to the observed first-order rate constant k_{obs}, which corresponds to $\Delta G_2^{\ddagger}(298) = 24.1(\pm 0.1)$ kcal mol^{-1}. Figure 5 presents the free energy profile for the interconversion of complexes **2** and **3**.

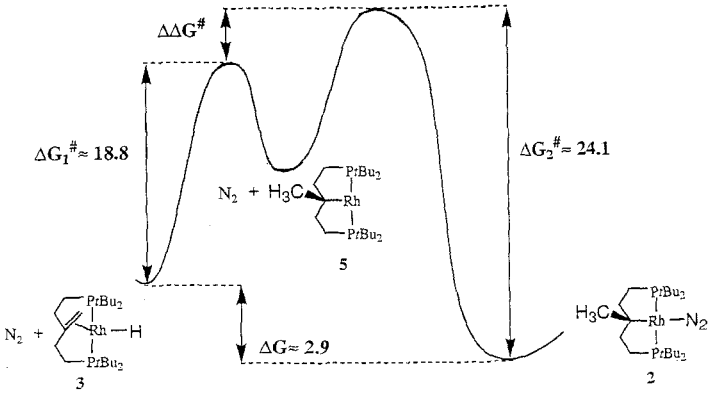

Figure 5. Free energy profile for the interconversion of complexes **2** and **3** (298 K, kcal mol^{-1}).

6. X-ray Crystal Structures of complexes 2 and 3: A red crystal was formed from a pentane solution of **2** and **3** (**2**:**3** = 7:3, by NMR) which was allowed to stand at room temperature. X-ray crystallographic analysis showed two species to be present in the crystal lattice, occupying the same crystallographic sites, in a 6:4 ratio, similar to the ratio in solution.[18] The crystal data for complexes **2** and **3** are presented in Table 4 (see Experimental Section). The molecular structures of **2** and **3** are shown in Figures 6 and 7, respectively. Bond lengths and angles for **2** and **3** are given in Table 3.

Table 3. Selected bond lengths (Å) and angles (°) for $\mathbf{2}_{0.6}\mathbf{3}_{0.4}$.

Rh1–P1	2.262(2)	Rh1–P2	2.290(2)
Rh1–N1	2.032(1)	Rh1–C3	2.135(5)
Rh1–C31a	2.17(2)	N1–N2	0.963(14)
C3–C31a	1.468(12)	C3–C31b	1.36(2)
P1-Rh1-P2	164.33(5)	P1-Rh1-N1	95.9(2)
P1-Rh1-C3	85.63(14)	P2-Rh1-N1	95.3(2)
P2-Rh1-C3	84.41(14)	N2-N1-Rh1	173.8(10)
N1-Rh1-C3	173.8(2)	C31a-C3-Rh1	73.1(7)

a) Crystal structure of complex **2**: As shown in Figure 6, complex **2** has a slightly distorted square-planar structure. The N1–N2 bond length of 0.963(14) Å is comparable with the those reported for $[ClRh(iPr_3P)_2(N_2)]$ (0.958(5) Å)[19] and $[HRh(tBu_2PPh)_2(N_2)]$ (1.074(7) Å),[20] and it is shorter than that of free N_2 (1.10 Å).[21] (The reasons for this bond contraction have been discussed.[22]) The P1-Rh1-P2 angle of 164.33(5)° is comparable to those reported for the similar Rh and Ir complexes $[HRhCl\{HC(CH_2CH_2P(tBu)_2)_2\}]$[8a] (167.8(2)°) and $[HIrCl\{HC(CH_2CH_2P(tBu)_2)_2\}]$[22] (167.5(1)°). The configuration around the *ipso* carbon atom is almost perfectly tetrahedral, indicating that there is no interaction between the Rh atom and the protons of the methyl group bound to the *ipso* carbon.

0947-6539/97/0302-0256 $ 15.00+.25/0 Chem. Eur. J. 1997, 3, No. 2

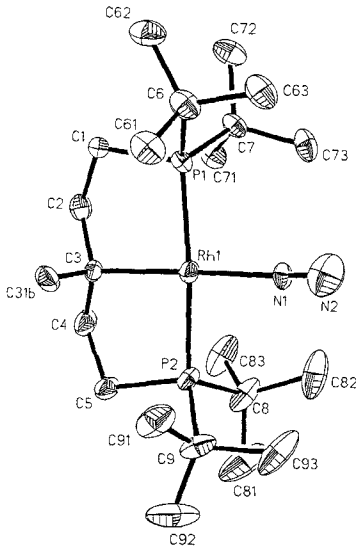

Figure 6. Molecule of **2** in the crystal (hydrogen atoms have been omitted for clarity).

b) Crystal structure of complex 3: Complex **3** (Figure 7) exhibits a C3–C31a double bond length of 1.36(2) Å, slightly longer than that of free ethylene (1.337(2) Å)[23] and within the range of other rhodium olefin complexes.[24, 25] Although the bond lengths Rh1–C3 and Rh1–C31a cannot be precisely compared since two complexes are present in the crystal lattice, the observed values (2.135(5) and 2.17(2) Å, respectively) together with the NMR data indicate that there is "slippage" of the rhodium atom towards the most substituted carbon of the double bond. The angle C31a-C3-Rh1 is 73.1(7)°, indicating that the double bond is distorted from an ideal *trans* configuration with respect to the hydride (the hydride was not located in the structure).

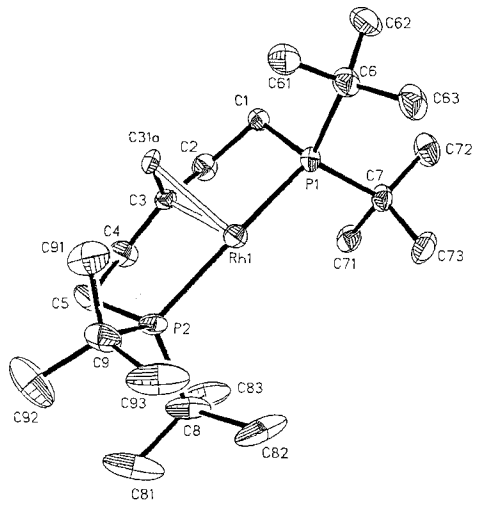

Figure 7. Molecule of **3** in the crystal (hydrogen atoms have been omitted for clarity).

Discussion

It is well established that hydride and olefinic protons can undergo rapid exchange in a metal coordination sphere via olefin insertion and β-hydrogen elimination processes. A concerted 4-centered mechanism is assumed for this type of reaction.[6, 26] All of the reported systems are postulated to involve *cis* insertion, while in our case *formally* direct *trans* insertion occurs. As in other reactions involving coordinated olefins, some "slippage" of the metal atom takes place at the stage prior to migration or nucleophilic attack,[27] resulting in a shift of the metal towards the *least* substituted carbon atom, unless some additional stabilization is provided by the substituents of the olefin (mainly heteroatoms). In our system the rhodium atom migrates *exclusively* to the *most substituted* quaternary carbon. This phenomenon is probably due to the presence of the two bulky phosphine groups which are held in position *trans* to each other by the rigid chelate core, favoring the formation of two 5-membered rings rather than two 6-membered ones.

The high stability of this bischelated system leads to another interesting question concerning the mechanism of hydride migration to the olefin. In the only previously reported study of olefin insertion into the Rh–H bond, it was assumed that hydride migration to the ethylene ligand in the square-planar d^8 rhodium complex *trans*-[HRh(iPr$_3$P)$_2$(C_2H_4)] proceeds via a *cis* intermediate.[4a] As mentioned in that work, the ease of the presumed *trans*-to-*cis* isomerization of this complex is surprising.[28]

In our system, hydride migration to the olefin is very unlikely to proceed through a *trans–cis* rearrangement. Both the bulkiness of the phosphines and the high stability of the two 5-membered planar chelates would disfavor this process. Coordination of a fifth ligand (solvent, N_2) to **3**, thereby enabling a *cis* olefin–hydride arrangement, is unlikely. Since the migratory insertion process takes place in such a noncoordinating unpolar solvent as cyclohexane, solvent coordination to **3** probably does not play a role in the mechanism. N_2 coordination to **3** is incompatible with the lack of magnetization transfer between **2** and **3**. No other species that could be assigned as the *cis* intermediate were observed by IR or by NMR spectroscopy. It appears that the structure of the hydrido–olefin complex **3** does not require this type of isomerization, since the C=C double bond plane does not lie perpendicularly to the Rh–H bond (the C=C–Rh angle is about 73°), and therefore, the necessary "*cis* arrangement" in the *transition state* can be achieved by a further shift in the position of the hydride. The P-Rh-P angle of 164.33(5)° represents an additional distortion from the ideal square-planar structure. All these factors may produce the necessary requirements for the direct "*trans*" hydride migration, without involvement of a *cis* complex, which would be unfavorable in the ideal case.[29] The high, negative value of the entropy of activation is also compatible with a highly organized late transition state, which is formed upon the distortion from planarity in **3**.

Hydride migration to an ethylene ligand in a *trans* position was reported in the complex *trans*-[(2,11-bis(diphenylphosphinomethyl)benzo[c]phenanthrene)PtH(C_2H_4)]$^+$.[30] It was proposed that a *cis* H–C_2H_4 orientation is obtained in this case by coordination of another ethylene molecule[30] or by distortion of the P-Pt-P angle.[29a]

It is noteworthy that the methyl olefin complex [RhCH$_3$-{CH$_2$=C(CH$_2$CH$_2$P(tBu)$_2$)$_2$}] (**6**), which we prepared by treatment of [RhCl{CH$_2$=C(CH$_2$CH$_2$P(tBu)$_2$)$_2$}][8] with MeLi in THF, does not undergo the migratory insertion process even when heated at 110 °C for days. Although hydride migration to an olefin ligand is faster,[31a] alkyl migration in rhodium *cis*-alkyl–olefin complexes can occur under relatively mild conditions.[31b, c] Were a classic *cis* intermediate to be formed in our system, methyl migration in **6** (if thermodynamically favorable) might have been expected.

It has been recently shown that an unsaturated metal–alkyl complex, formed upon hydride to olefin migration, is not neces-

sarily the species responsible for the observed hydrogen scrambling in a *cis* hydrido–olefin metal complex.[32] A detailed NMR study of some early transition metal complexes,[33] including reinvestigation of a study involving the niobium complex $[Cp_2Nb(CH_2{=}CHCH_3)H]$,[34] concluded that agostic interactions participate in the hydrogen exchange. Exploring these considerations in our system may lead to some intriguing questions: 1) If this type of intermediate does participate in our equilibrium, what should its geometry be? 2) What is the role of nitrogen in this process?

The kinetic data clearly shows that the dissociation of the dinitrogen ligand from complex **2** is the rate-determining step in the overall conversion of **2** to **3**. Based on this, and on the fact that the H_3C-C-Rh angle in **2** (104.2°) is very close to tetrahedral, we believe that formation of an 18-electron agostic intermediate *prior* to dissociation of the N_2 ligand is unlikely. In addition, the square-planar d^8 configuration is expected to be very stable. However, we have recently demonstrated that substitution of a dinitrogen ligand in a similar complex, **1a**, by a weaker ligand (CO_2) to form complex **1d** results in the appearance of a strong agostic interaction between the Rh atom and the proton attached to the *ipso* carbon.[5] The presence of an agostic interaction, even at the stage of the square-planar 16-electron complex **1d**, suggests that such an interaction would be even more favorable for a 14-electron intermediate formed upon dissociation of N_2 from **2**. It has been also demonstrated that associative formation of an agostic interaction can occur upon dissociation of a loosely bound ligand from the tungsten coordination sphere.[35] From this point of view, the unsaturated T-shaped 14-electron complex **5** probably does not exist as such, but rather has the agostic structure **5′** (Figure 8). The latter must be quite unstable, since its formation leads to substantial perturbations in the electronic structure (the geometry of **5′** must be strongly distorted from the square-planar configuration, resulting in a considerable increase in the free energy of the system). Therefore, **5′** undergoes facile β-hydrogen elimination giving **3**.[36] Rapid in-place rotation followed by β-hydrogen elimination results in the hydrogen scrambling observed for **3** (Figure 8).

Finally, we would like to point out the role of nitrogen in our process. Various small molecules are frequently used for trapping unsaturated intermediates in many migratory insertion processes involving metal centers. Carbon monoxide, phosphines, and nitriles are among the most common ones.[4a, 37] Practically all of them dramatically slow down the reverse reaction, playing a role of a reaction sink. The migratory insertion intermediate may also be trapped by a solvent molecule, although such adducts are normally very difficult to observe.[38] To our knowledge there are no examples of the use of atmospheric nitrogen as a trap for such a process. While dinitrogen can reversibly substitute various ligands from their metal complexes,[39] it is commonly used in many reactions requiring anaerobic conditions.[40] Here we have shown that nitrogen, even at low concentrations in solution, can easily trap the unsaturated species and shift the equilibria towards the insertion product. It is possible that dinitrogen may play a significant role in catalytic reactions performed under nitrogen and involving a slow migratory insertion step.

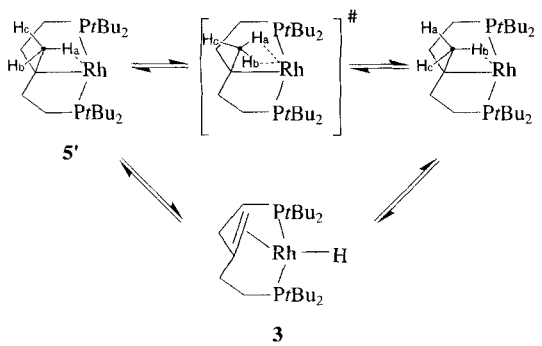

Figure 8. Proposed mechanism of hydrogen scrambling in complex **3**.

Conclusion

The thermally stable hydrido–olefin Rh complex $[RhH\{CH_2{=}C(CH_2CH_2P(tBu)_2)_2\}]$ (**3**) undergoes facile olefin insertion/β-hydrogen elimination processes. The structural data obtained from the NMR spectroscopy of **3** and its X-ray crystal structure, together with the high entropy of activation for the insertion reaction, as derived from the spin saturation transfer study ($\Delta S^{\neq} \approx -40$ e.u.), suggest that direct *trans* insertion takes place in this system. Although the theory disfavors such a process,[29] we should take into consideration that, owing to the unique geometry of **3**, some distortion from the *trans* configuration is already present in the ground state, and therefore, the high energy barrier predicted for the bending of the olefin toward the hydride is partially overcome.

Another interesting point is the role of free nitrogen in the system. It is found that, under a nitrogen atmosphere, complex **3** exists in equilibrium with the dinitrogen complex $[Rh(N_2)\{CH_3C(CH_2CH_2P(tBu)_2)_2\}]$ (**2**). It has been demonstrated that the dinitrogen molecule is capable of efficiently trapping the unsaturated intermediate, which is formed upon olefin insertion into the metal–hydride bond. The dinitrogen complex **2** is thermodynamically more stable than $3 + N_2$ ($\Delta G_{298} \approx -2.9$ kcal mol^{-1}) and **3** can be completely converted to **2** under moderate N_2 pressure. To our knowledge this is the first example of a dinitrogen effect on an insertion reaction. It is also noteworthy that N_2 dissociation from **2** has a substantially higher activation barrier than those for the migratory insertion and β-hydrogen elimination reactions. These facts are worth considering when studying organometallic reactions under free N_2.

Experimental Section

General Procedures: All operations with air-and moisture-sensitive compounds were performed in a nitrogen-filled glove box (Vacuum Atmospheres with an MO-40 purifier). All solvents were reagent grade or better. Pentane, benzene, and THF were distilled over sodium/benzophenone ketyl. All solvents were degassed and stored under high-purity nitrogen after distillation. All deuterated solvents (Aldrich) were stored under high-purity nitrogen on molecular sieves (3 Å). Sodium hydride was purchased from Merck as an 80% suspension in Paraffin oil and washed with pentane in a glove box until only traces of oil remained. ^1H, ^{31}P, and ^{13}C NMR spectra were recorded at 400, 162, and 100 MHz, respectively, using a Bruker AMX 400 spectrometer. ^1H and ^{13}C chemical shifts are reported relative to TMS and referenced to the residual solvent C_6D_5H ($\delta = 7.15$, benzene) and all-deuterated solvent peaks ($\delta = 128.00$, benzene), respectively. ^{31}P chemical shifts are relative to H_3PO_4 and referenced to an external 85% phosphoric acid sample. All measurements were performed at 23 °C unless otherwise specified.

0947-6539/97/0302-0258 $ 15.00+.25/0 Chem. Eur. J. 1997, 3, No. 2

Reaction of 4 with sodium hydride to form 2 and 3: To a solution of the rhodium hydrido chloride **4** (40 mg, 0.078 mmol) in THF (4 mL) was added NaH (30 mg 1.25 mmol). The suspension was vigorously stirred for 24 h at room temperature, after which it was filtered and the THF pumped off under vacuum. The resulting solid was dissolved in pentane, and the pentane solution filtered again to remove insoluble inorganic particles. A 1:1 mixture of **2** and **3** was obtained as an extremely air-sensitive dark red solid after evaporation of the pentane. Yield 34 mg. Bubbling dry argon through a warm solution containing **2** and **3** in benzene results in disappearance of **2** and quantitative formation of pure **3**. The assignments of signals due to **2** and **3** given below are confirmed by $^{13}C\{^1H\}$, ^1H–2D correlation and DEPT $^{13}C\{^1H\}$ experiments.

[Rh(N$_2$){CH$_3$C(CH$_2$CH$_2$P(*t*Bu)$_2$)$_2$}] (2): IR (film): $\tilde{\nu} = 2110\ cm^{-1}$ (s, (N≡N). $^{31}P\{^1H\}$NMR (C_6D_6): $\delta = 86.95$ (d, J(Rh–P) = 172.1 Hz). ^1H NMR (C_6D_6,): $\delta = 1.16$ (s, 3H), 1.27 (m of overlapped signals of **2** and **3**; appear as two singlets at $\delta = 1.30$ and 1.28 in $^1H\{^{31}P\}$ NMR, 36H). Other signals: $\delta = 1.8$ (m), 1.57 (m), 1.39 (m). $^{13}C\{^1H\}$ NMR (C_6D_6): $\delta = 55.6$ (dt, J(Rh–C) = 28.1 Hz, J(P–C) = 1.9 Hz, ipso-C). Other signals: $\delta = 24.08$ (td, J(P–C) = 7.0 Hz, J(Rh–C) = 3.0 Hz, CH_2–P), 36.22 (t, J(P–C) = 4.9 Hz, $CH_2(CH_2$–P)), 35.6 (td, J(P–C) = 5.8 Hz, J(Rh–C) = 0.7 Hz, $C(CH_3)_3$), 35.12 (td, J(P–C) = 5.7 Hz, J(Rh–C) = 1 Hz, $C(CH_3)_3$), 30.18 (m, *t*Bu CH_3), 27.66 (s, CH_3(C–Rh)).

[RhH{CH$_2$=C(CH$_2$CH$_2$P(*t*Bu)$_2$)$_2$}] (3): IR (film): $\tilde{\nu} = 1791\ cm^{-1}$, (br, Rh–H). Elemental analysis: calcd C 55.46, H 9.94; found C 55.71, H 10.06; $^{31}P\{^1H\}$ NMR (C_6D_6): $\delta = 86.71$ (brd, J(Rh–P) = 152.7 Hz). ^1H NMR (C_6D_6): $\delta = -3.16$ (dt, appears as a d in $^1H\{^{31}P\}$ NMR, J(Rh–H) = 21.0 Hz, J(P–H) = 19.3 Hz, 1H, hydride), 2.78 (brs, 2H, CH_2 of the olefin group), 1.27 (m, appears as two singlets at $\delta = 1.27$ and 1.26 in $^1H\{^{31}P\}$ NMR, 36H). Other signals: $\delta = 1.88$ (m, 4H), 1.7 (m, 2H), 1.54 (m, 2H). $^{13}C\{^1H\}$ NMR (C_6D_6): $\delta = 97.4$ (dt, J(Rh–C) = 9.8 Hz, J(P–C) = 3.6 Hz, quartenary carbon of the olefin group), 48.22 (dt, J(Rh–C) = 8.6 Hz, CH_2 of the olefin group, overlapped with $CH_2(CH_2$–P)). Other signals: $\delta = 24.08$ (t, J(P–C) = 4.4 Hz, CH_2–P), 48.19 (m, $CH_2(CH_2$–P)), 33.21 (td, J(P–C) = 7.7 Hz, J(Rh–C) = 3.4 Hz, $C(CH_3)_3$), 30.66 (t, J(P–C) = 3.2 Hz, *t*Bu CH_3), 30.36 (t, J(P–C) = 4.1 Hz, *t*Bu CH_3).

Synthesis of [RhCH$_3${CH$_2$=C(CH$_2$CH$_2$P(*t*Bu)$_2$)$_2$}] (6): To a solution of [RhCl{CH$_2$=C(CH$_2$CH$_2$P(*t*Bu)$_2$)$_2$}] [8] (23 mg, 0.045 mmol) in THF (3 ml) were added 35 μL of a 1.4 M solution of MeLi in diethyl ether at −30 °C. The solution immediately turned dark red. The reaction mixture was allowed to reach room temperature and solvent was evaporated. Pentane (3 mL) was added to the resulting solid, and the precipitate was isolated by filtration, washed with 2 × 2 mL of pentane, and the washings combined with the filtrate. After removal of the solvent under vacuum, **6** was obtained as a air-sensitive red solid. Yield 21 mg (95.5%). Elemental analysis: calcd C 56.32, H 10.07; found C 55.38, H 9.58. $^{31}P\{^1H\}$ NMR (C_6D_6): $\delta = 62.50$ (d, J(Rh–P) = 153.3 Hz). ^1H NMR (C_6D_6): $\delta = 1.13$ (td, J(P–H) = 5.8 Hz, J(Rh–H) = 1.9 Hz, 3H, CH_3), 2.58 (brs, 2H, CH_2 of the olefin), 1.29 (vt, J(P–H) = 5.8 Hz, singlet in $^1H\{^{31}P\}$ spectrum, 18H, *t*Bu), 1.27 (vt, J(P–H) = 5.7 Hz, singlet in $^1H\{^{31}P\}$ spectrum, 18H, *t*Bu). Other signals: $\delta = 1.90$ (m, 4H), 1.70 (m, 2H), 1.50 (m, 2H). $^{13}C\{^1H\}$ NMR (C_6D_6): $\delta = 87.48$ (dt, J(Rh–C) = 9.1 Hz, J(P–C) = 3.4 Hz, quartenary carbon of the olefin group), 45.88 (dt, J(Rh–C) = 8.6 Hz, J(P–C) = 2.1 Hz, CH_2 of the olefin group), −7.03 (dt, J(Rh–C) = 23.3 Hz, J(P–C) = 11.6 Hz, CH_3). Other signals: $\delta = 34.96$ (t, J(P–C) = 4.1 Hz, $CH_2(CH_2$–P)), 20.15 (t, J(P–C) = 5.9 Hz, CH_2–P), 35.89 (m, $C(CH_3)_3$), 31.22 (t, J(P–C) = 2.8 Hz, CH_3 of *t*Bu group), 30.12 (t, J(P–C) = 3.4 Hz, CH_3 of *t*Bu group).

Measurement of olefin insertion rate with the saturation transfer technique: All the experiments were performed in a screw-capped NMR tube. In a typical experiment, an NMR tube was loaded with an approximately 1:1 mixture of **2** and **3** (ca. 25 mg) in 0.5 mL of [D$_8$]dioxane in the glove box and then placed in a Bruker AMX400 spectrometer. The measurement temperature was kept constant (±0.2 °C) throughout the experiment. Equilibrium was reached within several minutes ($^{31}P\{^1H\}$ NMR). No other species or decomposition products were observed. Saturation transfer experiments were performed by selective saturation of the hydride resonance under steady state conditions. The response of the signal of the olefinic protons was detected by comparison with a control experiment (the signal-free area was irradiated under the same conditions). The relaxation time (T_{obs}) of the olefinic protons was measured using the standard inversion-recovery technique combined with the saturation of the hydride resonance. The k_{obs} value was calculated from the saturation transfer (Forsen–Hoffman) equation: $I^{\infty}/I^{c} = T_{obs}/(T_{obs} + k_{obs})$, where I^{∞} is the intensity of the signal of the olefinic protons under the saturation of the hydride resonance and I^{c} is the intensity from the control experiment [15b].

Measurement of N$_2$ dissociation rate from 2: In a typical experiment, 16 mg of an approximately 1:1 mixture of **2** and **3** in 1.2 mL of benzene was placed in a 10 mm high-pressure NMR tube (Wilmad 513-7PVH), and the solution was pressurized with 80 psi N_2. The mixture was allowed to reach an equilibrium ratio between **2** and **3** (ca. 5:1). The dinitrogen pressure was released and the tube shaken well to ensure that no extra gas pressure remained (the system was opened and closed twice). The $^{31}P\{^1H\}$ NMR spectrum showed that there was no dramatic ratio change occured between **2** and **3** upon the release of the pressure. The first kinetic spectrum was obtained after 45 min from the beginning of the experiment.

Data Collection and the X-ray Structure Determination of 2 and 3: A red block of approximate dimensions 0.3 × 0.3 × 0.2 mm was mounted on a glass fiber using silicone grease and placed on a Rigaku AFC5R diffractometer. Data was collected at 110 K. The unit cell was obtained by a random search of 20 carefully centered reflections in the 2θ range of 8.0–25.0°. Monitoring of three standard reflections (*hkl*: 0 −2 −2, 1 2 −4, 1 −3 −2) every 200 reflections indicated no decay of the crystal in the X-ray beam. Data were collected at constant scan speed (16° min^{-1}) in the Ω scan mode in two shells [range: a) $2<2\theta<44°$, b) $44<2\theta<55°$) ($-15<h<15$, $0<k<18$, $-3<l<19$). The data were corrected for Lorentz and polarization effects. The data was not corrected for absorption due to the low absorption ($\mu = 0.811\ mm^{-1}$) of the crystal. A summary of the data collection information is given in Table 4. The structure was solved by a Patterson map (SHELXS86) and then expanded using Fourier methods and refined by full-matrix least squares refinement (SHELXL93) (5816 reflections with $I > 2\sigma(I)$; $R1 = 0.0621$, $wR2 = 0.1421$). Scattering factors and corrections for anomalous dispersion were those implemented in the SHELX program package. The solution showed two species to be present in the crystal lattice, occupying the same crystallographic sites in a 6:4 ratio. This ratio was also verified by $^{31}P\{^1H\}$ NMR, which gave a slightly different ratio (7:3). All non-hydrogen atoms were refined with anisotropic temperature factors. The *t*Bu groups have slightly higher temperature factors due to high thermal motion, common for *t*Bu groups. The hydrogen atoms were included in the structure factor calculations at the final stage using a riding model with

Table 4. Crystal data for **2**$_{0.6}$**3**$_{0.4}$.

formula	$C_{22}H_{47}N_{1.2}P_2Rh$
M_r	493.3
space group	$P2_1/c$
a/Å	12.173(2)
b/Å	14.121(3)
c/Å	15.367(3)
β/°	106.50(3)
V/Å^3	2532.7(8)
Z	4
ρ_{calcd}/g cm^{-3}	1.326
cryst. size/mm	0.2 × 0.3 × 0.3
F(000)	1076
$\mu(Mo_{K\alpha})$/mm^{-1}	0.811
instrument	Rigaku AFC5R
radiation (monochromated incident beam)	$Mo_{K\alpha}$
orientation reflns, no.	3
T/K	110
scan method	Ω
data collection range (θ)/°	1.74–27.51
data collected, unique, total obs.	7440, 5818, 5793 ($F > 4\sigma(F)$)
parameters refined	264
$R1$, $wR2$ [a]	6.21, 14.21
$R1$, $wR2$ (all data)	8.57, 16.47
GOF	1.061
largest peak, hole/e Å^{-3}	0.827, −0.974

[a] $w = 1/[\sigma^2(F_o^2) + (0.0637P)^2 + 8.0269P]$, where $P = (F_o^2 + 2F_c^2)$.

d(C–H) = 0.98 Å for the bonded carbon atoms. Hydrogens were introduced at calculated positions around the methyl C31b with 0.6 occupancy. In the final difference map, the largest peak (0.827 e Å^{-3}) and hole (– 0.974 e Å^{-3}) appeared in close proximity around the rhodium center (ca. 0.4–0.6 Å) and could not be interpreted in a chemically significant way. Bond lengths and angles are given in Table 3. The molecular structures of **2** and **3** are shown in Figures 6 and 7, respectively.

Crystallographic data (excluding structure factors) for the structures reported in this paper have been deposited with the Cambridge Crystallographic Data Centre as supplementary publication no. CCDC-100055. Copies of the data can be obtained free of charge on application to The Director, CCDC, 12 Union Road, Cambridge CB21EZ, UK (Fax: Int. code +(1223)336-033; e-mail: teched@chemcrys.cam.ac.uk).

Acknowledgements: This work was supported by the Israel Science Foundation, Jerusalem, Israel. A. V. thanks the Ministry of Science and the Arts for a fellowship. H-B. K. thanks the MINERVA foundation, Munich, Germany, for a postdoctoral fellowship. D. M. is the holder of the Israel Matz professorial chair of organic chemistry.

Received: August 22, 1996 [F448]

[1] G. W. Parshall, S. D. Ittel, *Homogeneous Catalysis*, 2nd ed., **1992**, Wiley, New York.

[2] a) N. M. Doherty, J. E. Bercaw, *J. Am. Chem. Soc.* **1985**, *107*, 2670–2682; b) B. J. Burger, B. D. Santarsiero, M. S. Trimmer, J. E. Bercaw, *ibid.* **1988**, *110*, 3134–3146; c) H. E. Bunting, M. L. H. Green, P. A. Newman, *J. Chem. Soc. Dalton Trans.* **1988**, 557–577; d) J. P. McNally, N. J. Cooper, *Organometallics* **1988**, *7*, 1704–1715; e) J. W. Byrne, H. U. Blaser, J. A. Osborn, *J. Am. Chem. Soc.* **1975**, *97*, 3871–3873.

[3] a) H. Werner, R. Feser, *Angew. Chem. Int. Ed. Engl.* **1979**, *18*, 157–158; b) H. Werner, R. Feser, *J. Organomet. Chem.* **1982**, *232*, 351–370; c) J. Halpern, T. Okamoto, *Inorg. Chim. Acta* **1984**, *89*, L53–54; d) A. J. Deeming, B. F. G. Johnson, J. Lewis, *J. Chem. Soc. Dalton Trans.* **1973**, 1848–1852; e) H.-F. Klein, R. Hammer, J. Gross, U. Schubert, *Angew. Chem. Int. Ed. Engl.* **1980**, *19*, 809–810; f) J. R. Brown, P. L. Evans, A. R. Lucy, *J. Chem. Soc. Perkin Trans. II* **1987**, 1589–1596; g) B. Olgemoller, W. Beck, *Angew. Chem. Int. Ed. Engl.* **1980**, *19*, 834; h) E. G. Lundquist, K. Folting, W. E. Streib, J. C. Huffman, O. Eisenstein, K. G. Caulton, *J. Am. Chem. Soc.* **1990**, *112*, 855–863; i) L. P. Seiwell, *Inorg. Chem.* **1976**, *15*, 2560–2563.

[4] We are aware of only one example where olefin insertion into a metal–hydride bond in such complexes was studied in detail: a) D. C. Roe, *J. Am. Chem. Soc.* **1983**, *105*, 7770–7771; b) Although less relevant, a study of a Ru^{II} complex in a similar system was also reported: B. N. Chaudret, D. J. Cole-Hamilton, G. Wilkinson, *Acta Chem. Scand. A* **1978**, *32*, 763–769. c) Spectral data of a *saturated* hydrido–olefin rhodium(I) complex were reported in: C. Bianchini, C. Mealli, A. Meli, Sabat, M. *J. Chem. Soc. Chem. Commun.* **1986**, 777–779.

[5] A. Vigalok, Y. Ben-David, D. Milstein, *Organometallics* **1996**, *15*, 1838–1844.

[6] See, for example: J. P. Collman, L. S. Hegedus, J. R. Norton, R. G. Finke, *Principles and Applications of Organotransition Metal Chemistry*, University Science Books, Mill Valley, California, **1987**.

[7] For a quantitative study of this type of reaction see also: H. E. Bryndza, *J. Chem. Soc. Chem. Commun.* **1985**, 1696–1698.

[8] a) C. Crocker, R. J. Errington, W. S. McDonald, K. J. Odell, B. L. Shaw, R. J. Goodfellow, *J. Chem. Soc. Chem. Commun.* **1979**, 498–499; b) C. Crocker, R. J. Errington, R. Markham, C. J. Moulton, K. J. Odell, B. L. Shaw, *J. Am. Chem. Soc.* **1980**, *102*, 4373–4379.

[9] For a review see: G. L. Geoffrey, J. R. Lehman, *Advances in Inorg. and Radiochem.* **1977**, 189–290.

[10] a) J. Chatt, R. S. Coffey, B. L. Shaw, *J. Chem. Soc.* **1965**, 7391–7402; b) L. Malatesta, *J. Am. Chem. Soc.* **1979**, *101*, 3987–3989 and references cited therein.

[11] A. L. Seligson, W. C. Trogler, *Organometallics* **1993**, *12*, 738–743.

[12] A. Seidell, *Solubilities of Inorganic and Metal Organic Compounds*, 3rd ed., Van Nostrand, New York, NY, **1940**, and supplements.

[13] The nitrogen solubility at various temperatures can be calculated with the known solubility and ΔH of solubilization at 298.15 K, see: E. Wilhelm, R. Battino, *Chem. Rev.* **1973**, *73*, 1–9.

[14] Examples of negative NOE values are very scarce. See: P. Balaram, A. A. Bothner-By, J. Dadok, *J. Am. Chem. Soc.* **1979**, *101*, 4015–4016.

[15] a) The use of saturation transfer kinetics is limited to slow exchange processes, where the relaxation times of the nuclei involved are comparable with the rate constants, see ref. [15b]; b) L.-Y. Lian, G. C. K Roberts, in *NMR of Macromolecules*, Roberts, (Ed: G. C. K. Roberts) The Practical Approach Series, IRL Press, Oxford University Press, **1993**, pp. 153–182; c) The method has been recently applied for the exchange between a hydride and an agostic hydrogen atom in a ruthenium coordination sphere: M. Ogasawara, M. Saburi, *Organometallics* **1994**, *13*, 1911–1917.

[16] S. Forsen, R. A. Hoffman, *J. Chem. Phys.* **1964**, *40*, 1189–1196.

[17] M. L. H. Green, L.-L. Wong, A. Sella, *Organometallics* **1992**, *11*, 2660–2668.

[18] Other examples of two similar metal complexes co-crystallizing within one crystal lattice are reported: a) D. Coucouvanis, S. Al-Ahmad, C. G. Kim, S.-M. Koo, *Inorg. Chem.* **1992**, *31*, 2996–2998; b) W. Purcell, S. S. Bason, J. G. Leipoldt, A. Roodt, H. Preston, *Inorg. Chim. Acta* **1995**, *234*, 153–156.

[19] D. L. Thorn, T. H. Tulip, J. A. Ibers, *J. Chem. Soc. Dalton Trans.* **1979**, 2022–2025.

[20] P. R. Hoffman, T. Yoshida, T. Okano, S. Otsuka, J. A. Ibers, *Inorg. Chem.* **1976**, *15*, 2462–2466.

[21] A. J. Gordon, R. A. Ford, *The Chemist's Companion*, Wiley & Sons, NY, **1972**.

[22] C. Crocker, H. D. Empsall, R. J. Errington, E. M. Hyde, W. S. McDonald, R. Markham, M. C. Norton, B. L. Shaw, B. Weeks, *J. Chem. Soc. Dalton Trans.* **1982**, 1217–1224.

[23] L. S. Bartell, E. A. Roth, C. D. Hollowell, K. Kuchitzu, J. E. Young, *J. Chem. Phys.* **1965**, *42*, 2683–2686.

[24] C. Busetto, A. D'Alfonso, F. Maspero, G. Perego, A. Zazzetta, *J. Chem. Soc. Dalton Trans.*, **1977**, 1828–1834.

[25] R. Mason, G. R. Scollary, *Aust. J. Chem.* **1978**, *31*, 781–789.

[26] A. Nakamura, S. Otsuka, *J. Am. Chem. Soc.* **1973**, *95*, 7262–7272.

[27] An excellent example of hydride migration to an asymmetrically-bound ethylene molecule has been reported: J. W. Byrne, J. R. H. Kress, J. A. Osborn, L. Ricard, R. E. Weiss, *J. Chem. Soc. Chem. Comm.* **1977**, 662–663.

[28] The reported coupling constant ^2J(P–P) = 193 Hz for the proposed *cis* intermediate (low-temperature observation) is somewhat unusual for a square-planar system having two magnetically nonequivalent phosphorus atoms in *cis* positions to each other, which normally does not exceed 70 Hz. See, for example: K. Wong, G. P. Rosini, S. P. Nolan, A. S. Goldman, *J. Am. Chem. Soc.* **1995**, *117*, 5082–5088.

[29] a) D. L. Thorn, R. Hoffmann, *J. Am. Chem. Soc.* **1978**, *100*, 2079–2090; b) See also, N. Koga, K. Morokuma, in *Transition Metal Hydrides* (Ed.: Dedieu), VCH: New York, **1992**. Chapt. 6.

[30] G. Bracher, P. S. Pregosin, L. M. Venanzi, *Angew. Chem. Int. Ed. Engl.* **1975**, *14*, 563–564.

[31] a) G. Parkin, G. Bunel, B. J. Burger, M. S. Trimmer, A. Van Asselt, J. E. Bercaw, *J. Mol. Catal.* **1987**, *41*, 21–39; b) M. Brookhart, D. M. Lincoln, *J. Am. Chem. Soc.* **1988**, *110*, 8719–8720; c) M. Brookhart, E. Hauptman, D. M. Lincoln, *ibid.* **1992**, *114*, 10394–10401.

[32] A. E. Derome, M. L. H. Green, L.-L. Wong, *New J. Chem.* **1989**, *13*, 747–753 and references therein.

[33] M. L. H. Green, L.-L. Wong, *J. Chem. Soc. Chem. Commun.* **1988**, 677–678.

[34] J. E. Bercaw, B. J. Burger, M. L. H. Green, B. D. Santasiero, A. Sella, M. S. Trimmer, L.-L. Wong, *J. Chem. Soc. Chem. Commun.* **1989**, 734–736.

[35] a) A. A. Gonzales, K. Zhang, S. P. Nolan, R. L. de la Vega, S. L. Mukerjee, C. D. Hoff, G. J. Kubas, *Organometallics* **1988**, *7*, 2429–2435; b) K. Zhang, A. A. Gonzales, S. L. Mukerjee, S.-J. Chou, C. D. Hoff, K. A. Kubat-Martin, D. Barnhart, G. J. Kubas, *J. Am. Chem. Soc.* **1991**, *113*, 9170–9176.

[36] a) The synthesis and characterization of this "transition state-like" complex were reported: R. B. Cracknell, A. G. Orpen, J. L. Spencer, *J. Chem. Soc. Chem. Commun.* **1984**, 326–328; b) For theoretical study see: N. Koga, S. Obara, K. Kitaura, K. Morokuma, *J. Am. Chem. Soc.* **1985**, *107*, 7109–7116.

[37] M. L. H. Green, L.-L. Wong, *J. Chem. Soc. Chem. Commun.* **1984**, 1442–1443.

[38] K. Nicholas, S. Raghu, M. Rosenblum, *J. Organomet. Chem.* **1974**, *78*, 133–137.

[39] For reviews see: a) J. Chatt, J. R. Dilworth, R. L. Richards, *Chem. Rev.* **1978**, *78*, 589–625; b) A. D. Allen, R. O. Harris, B. R. Loescher, J. R. Stevens, R. N. Whiteley, *Chem. Rev.* **1973**, *73*, 11–20; c) M. Hidai, Y. Mizobe, *Chem. Rev.* **1995**, *95*, 1115–1133 and references therein.

[40] It has been recently shown that, due to strong competition between dinitrogen and other incoming ligands, a catalytic cycle based on the formation of an unsaturated metal complex can be retarded by performing the reactions under a dinitrogen atmosphere: C. Bianchini, E. Farnetti, M. Graziani, M. Peruzzini, A. Polo, *Organometallics* **1993**, *12*, 3753–3761.

 0947-6539/97/0302-0260 $ 15.00+.25/0